Inorganica Chimica Acta 363 (2010) 3784–3789

Contents lists available at ScienceDirect

Inorganica Chimica Acta

journal homepage: www.elsevier.com/locate/ica

Syntheses, crystal structures and magnetic properties of 1D and 2D cobaltous coordination polymers with mixed ligands

Shi-Yuan Zhang [a], Zhen-Jie Zhang [a], Wei Shi [a,b,*], Bin Zhao [a,b], Peng Cheng [a]

[a] Department of Chemistry, Nankai University, Tianjin 300071, PR China
[b] State Key Laboratory of Coordination Chemistry, Nanjing University, Nanjing 210093, PR China

ARTICLE INFO

Article history:
Received 25 December 2009
Received in revised form 15 May 2010
Accepted 19 May 2010
Available online 26 May 2010

Keywords:
Coordination polymers
Co(II) complexes
Crystal structures
Magnetic properties
Hydrothermal synthesis

ABSTRACT

Two new Co(II) coordination polymers with mixed ligands, $\{[Co(BTA)_{0.5}(DBI)_2]\cdot DBI\cdot H_2O\}_n$ (**1**) and $[Co(PDA)(DBI)(H_2O)]_n$ (**2**) (H_4BTA = benzene-1,2,4,5-tetracarboxylic acid; H_2PDA = 2,2′-(1,2-phenylene)diacetic acid; DBI = 5,6-dimethyl-1*H*-benzoimidazole) have been synthesized under hydrothermal conditions, respectively. Both of them are characterized by elemental analyses, powder X-ray diffraction, thermogravimetric analysis, single-crystal X-ray diffraction, and magnetic susceptibilities. In **1**, the Co(II) ions are four-coordinated and lie in distorted tetrahedron coordination environment. 1D ladder-like chain structure is formed by the bridging BTA^{4-} ligand. In **2**, the Co(II) ions are in slightly distorted octahedral coordination geometry, and linked by PDA^{2-} ligand exhibiting a 2D layer structure. Temperature-dependent magnetic susceptibility measurements of **1** and **2** revealed that there are antiferromagnetic interactions between Co(II) ions.

1. Introduction

The fields of crystal engineering have been developed rapidly [1–4], because of the intriguing structural motifs and potential applications [5–11]. Recently, much attention has been given to the construction of coordination polymers (CPs) with interesting magnetic properties. To obtain such CPs, Co(II) ions are widely chosen as node to expand the structure for not only the variable geometric conformations including square-planar, tetrahedral, trigonal-bipyramid, octahedral and square-pyramidal among the first-row transition metal ions, but also the unquenched orbital contribution to magnetic moment with anisotropy [12–16]. Various Co(II) magnetic units containing monomers, dimers, polymers, chains, ladders, layers and 3D-networks have been synthesized and characterized due to their interesting magnetic properties such as ferromagnetic interactions, single molecule magnets or single chain magnets behaviors, etc [17–19]. On the other hand, it is important to select appropriate ligands to synthesize new coordination polymers for the study of magneto-structural relationship because: (i) Deliberately change of the interactions between metal ions and ligands can dramatically result in different magnetic properties [20–22]. (ii) Intermolecular interactions such as hydrogen bonds, π–π stacking, host–guest ionic interactions can significantly affect the magnetic interactions [23,24]. Among the numerous organic ligands, aromatic acids were given special interest for the abundant coordination modes and appropriate abilities to transfer ferro/antiferromagnetic interactions. Meanwhile, the use of neutral auxiliary ligands such as N-donor ligands to the synthetic system of aromatic acids with metal ions is helpful to construct specific structures with interesting properties. In this contribution, two new coordination polymers with mixed ligands $\{[Co(BTA)_{0.5}(DBI)_2]\cdot DBI\cdot H_2O\}_n$ (**1**) and $[Co(PDA)(DBI)(H_2O)]_n$ (**2**) (H_4BTA = benzene-1,2,4,5-tetracarboxylic acid; H_2PDA = 2,2′-(1,2-phenylene)diacetic acid; DBI = 5,6-dimethyl-1*H*-benzoimidazole) were synthesized under hydrothermal conditions and characterized by elemental analyses, PXRD, TGA, single-crystal X-ray diffraction, and magnetic susceptibilities. Magnetic studies of **1** and **2** revealed that there are antiferromagnetic interactions between Co(II) ions.

2. Experimental

2.1. General remarks

All reagents and solvents employed were commercially available and used as received without further purification.

Elemental analyses for C, H and N were carried out by using a Perkin–Elmer 240 CHN Elemental Analyzer. Infrared spectra were recorded on a TENOR 27 spectrophotometer as KBr pellets in the range 4000–400 cm^{-1}. Magnetic susceptibility measurements were performed in the range of 2–300 K with an applied dc field of 1000 Oe on a Quantum Design MPMS XL-7 SQUID system. The

---

* Corresponding author at: Department of Chemistry, Nankai University, Tianjin 300071, PR China. Tel.: +86 22 23503059; fax: +86 22 23502458.
E-mail address: shiwei@nankai.edu.cn (W. Shi).

0020-1693/$ - see front matter © 2010 Elsevier B.V. All rights reserved.
doi:10.1016/j.ica.2010.05.041

powder X-ray diffraction (PXRD) data were collected on a Rigaku D/max-250 diffractometer with Cu Ka radiation, and the recording speed was 0.2°/min over the 2θ range of 3–80° at room temperature. The thermogravimetric analyses were measured by a DSC-TG-DMA system from room temperature to 800 °C.

2.2. Preparations of the coordination polymers

A mixture of $Co(NO_3)_2{\cdot}6H_2O$ (0.4 mmol, 0.1164 g), DBI (0.1 mmol, 0.0146 g), H_4BTA (0.1 mmol, 0.0254 g) and water (10 mL) was sealed in a 25 mL Teflon-lined stainless steel vessel and heated at 150 °C for 2 days, and then cooled to room temperature at a rate of 10 °C/h. Red block-shaped crystals of **1** were collected, washed with distilled water, and dried in air. Yield: 56% based on $Co(NO_3)_2{\cdot}6H_2O$. Elemental analysis (%) *Anal* Calc. for **1**: C, 66.08; H, 5.72; N, 14.45. Found: C, 65.83; H, 5.13; N, 14.19%. IR data (KBr pellets, cm^{-1}): 3417m, 3132m, 1591s, 1476m, 1418m, 1401m, 1351s, 1309m, 1269m, 1136w, 1086w, 1004w, 973w, 820m, 613w, 518w.

2 was prepared by a procedure similar to that of **1** using H_2PDA (0.1 mmol, 0.0146 g) instead of H_4BTA. Yield: 61% based on $Co(NO_3)_2{\cdot}6H_2O$. Elemental analysis (%) *Anal* Calc. for **2**: C, 64.22; H, 5.39; N, 7.88. Found: C, 64.75; H, 5.06; N, 7.86%. IR data (KBr pellets, cm^{-1}): 3191s, 2362w, 1542s, 1506m, 1427m, 1399s, 1166w, 842w, 727m, 615m, 426w.

2.3. X-ray crystallography

Single-crystal analyses were performed on Oxford Supernova CCD diffractometer for **1** and Rigaku Saturn 007 CCD diffractometer for **2** with Mo Kα radiation (λ = 0.71073 Å) by the ω–φ scan technique. All data were collected for absorption by semiempirical method. The structures were solved primarily by direct method and secondly by Fourier difference techniques and refined by the full-matrix least-squares method. The computations were performed with the SHELXL-97 program [25,26]. All non-hydrogen atoms were refined anisotropically. The hydrogen atoms of organic ligands were set in calculated positions and refined as riding atoms with a common fixed isotropic thermal parameter. Crystallographic parameters and structural refinement for **1** and **2** are summarized in Table 1. Selected bond lengths and angles are listed in Table 2.

Table 1
Crystallographic data for **1** and **2**.

	1	**2**
Formula	$C_{32}H_{33}CoN_6O_5$	$C_{19}H_{19}CoN_2O_5$
Formula weight	640.57	414.29
T (K)	293(2)	293(2)
λ (Å)	0.71073	0.71073
Crystal system	triclinic	monoclinic
Space group	$P\bar{1}$	$C2/c$
a (Å)	9.5713(6)	33.406(7)
b (Å)	11.1182(7)	7.3968(15)
c (Å)	14.4993(10)	14.920(3)
α (°)	76.926(5)	90
β (°)	85.764(5)	108.53(3)
γ (°)	82.410(5)	90
V ($Å^3$)	1488.24(16)	3495.7(12)
Z	2	8
D_{calc} ($g\ cm^{-3}$)	1.429	1.574
F(0 0 0)	668	1712
Reflections collected	9925	14542
Unique reflections (R_{int})	5260 (0.0451)	4149 (0.0506)
θ Range (°)	2.53–25.10	2.57–27.86
Goodness-of-fit (GOF) on F^2	1.047	1.116
R^a, $R_w{}^b$ [$I > 2\sigma(I)$]	0.0644, 0.1484	0.0562, 0.1298
R^a, $R_w{}^b$ (all data)	0.0857, 0.1555	0.0679, 0.1372

[a] $R_1 = \sum||F_o| - |F_c||/\sum|F_o|$.

[b] $wR_2 = [w(|F_o{}^2| - |F_c{}^2|)^2/w|F_o{}^2|^2]^{1/2}$. $w = 1/[\sigma^2(F_o)^2 + 0.0297P^2 + 27.5680P]$, where $P = (F_o{}^2 + 2\,F_c{}^2)/3$.

3. Results and discussion

3.1. Synthesis

The preparation of **1** can be achieved via the 4:1:1 reaction of Co(II) nitrate hexahydrate, DBI and H_4BTA in aqueous solution by using hydrothermal method. In the same manner **2** was obtained using H_2PDA instead of H_4BTA. The crystal structures show great differences (1D ladder-like chain versus 2D layer), which may be caused by both the flexibility of the aromatic acid and the coordinated mode of the carboxylate groups [27,28].

3.2. Crystal structure of $\{[Co(BTA)_{0.5}(DBI)_2]{\cdot}(DBI){\cdot}(H_2O)\}_n$ (*1*)

1 crystallizes in the triclinic $P\bar{1}$ space group, each Co(II) ion is four-coordinated via two N atoms of DBI and two O atoms of two carboxylate groups from BTA^{4-} to form a distorted tetrahedron geometry as shown in Fig. 1(a). The Co–O bond lengths are 1.968(4) and 2.011(4) Å, while the lengths of Co–N are 2.004(5) and 2.041(5) Å, respectively. Each BTA^{4-} anion acts as a four-donated linker that connects four Co(II) ions, where two carboxylate

Table 2
Selected bond lengths (Å) and angles (°) for **1** and **2**.

1					
Co(1)–O(1)	1.971(3)	Co(1)–N(1)	2.002(3)	Co(1)–O(3)#1	2.009(3)
Co(1)–N(3)	2.045(3)	O(1)–Co(1)–N(1)	116.07(14)	O(1)–Co(1)–O(3)#1	100.94(12)
N(1)–Co(1)–	O(3)#1		111.85(13)	O(1)–Co(1)–N(3)	120.41(14)
N(1)–Co(1)–N(3)	107.36(14)				
O(3)#1–Co(1)–N(3)	98.43(13)				
2					
Co(1)–	O(2)#1	2.065(2)	Co(1)–O(1)	2.082(2)	Co(1)–N(1)
2.104(2)					
Co(1)–O(5)	2.107(2)	Co(1)–O(4)#2	2.157(2)	Co(1)–O(3)#2	2.226(2)
O(2)#1–Co(1)–O(1)	94.47(8)	O(2)#1–Co(1)–N(1)	94.40(9)	O(1)–Co(1)–N(1)	87.86(9)
O(2)#1–Co(1)–O(5)	88.22(8)	O(1)–Co(1)–O(5)	95.29(8)	N(1)–Co(1)–O(5)	175.75(9)
O(2)#1–Co(1)–	O(4)#2	98.31(8)	O(1)–Co(1)–O(4)#2	167.20(8)	N(1)–Co(1)–O(4)#2
90.39(9)					
O(5)–Co(1)–	O(4)#2	85.91(8)	O(2)#1–Co(1)–O(3)#2	156.99(8)	O(1)–Co(1)–O(3)#2
107.30(8)					
N(1)–Co(1)–	O(3)#2	93.80(8)	O(5)–Co(1)–O(3)#2	82.54(8)	O(4)#2–Co(1)–O(3)#2
60.16(7)					

Symmetry transformations used to generate equivalent atoms: for **1**: #1 $-x + 1, -y, -z + 1$; For **2**: #1 $-x + 1/2, y + 1/2, -z + 1/2$ #2 $-x + 1/2, -y + 3/2, -z$.

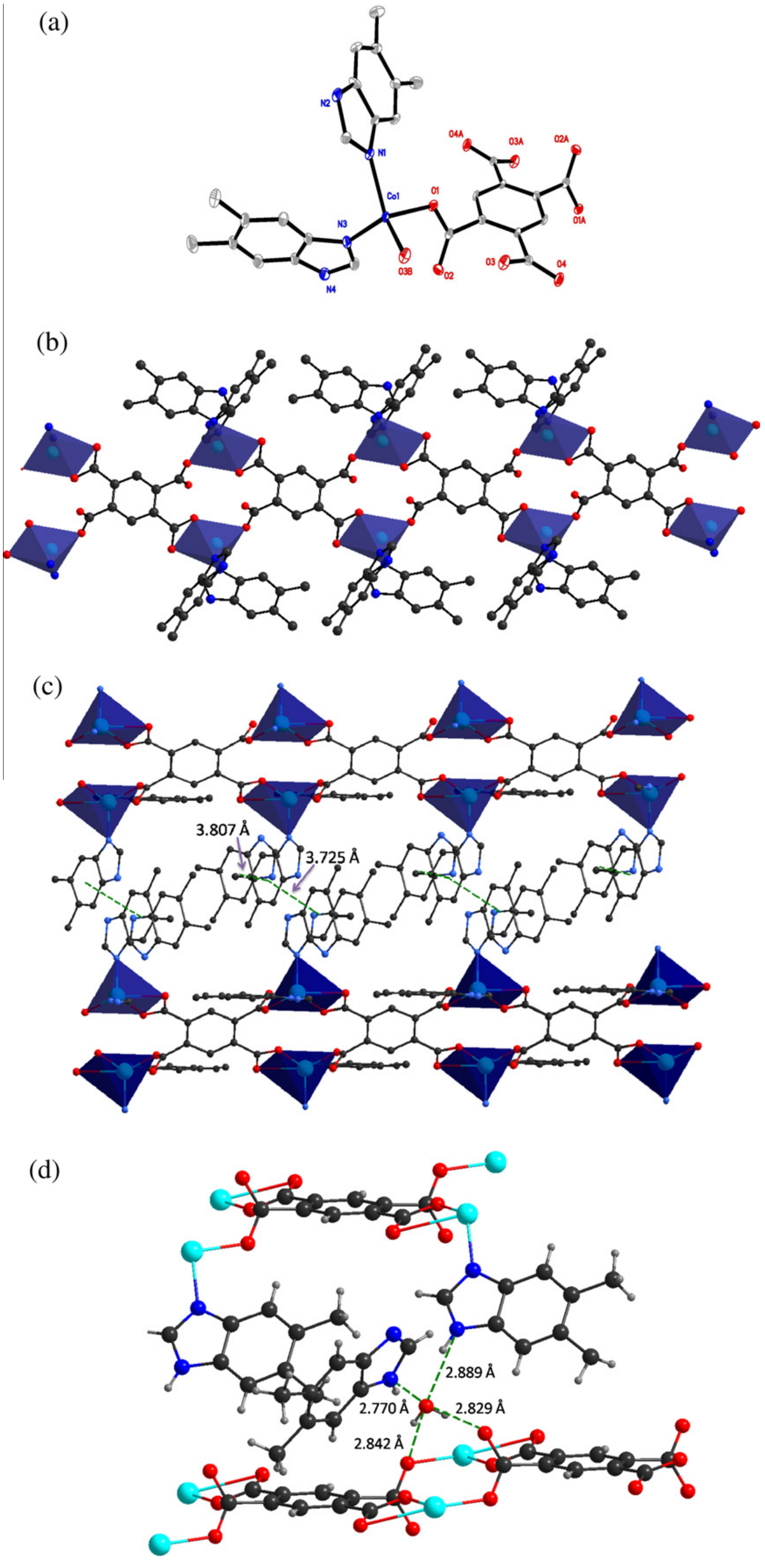

Fig. 1. (a) The coordination environment of Co(II) ions in **1**. (b) The 1D ladder-like chain of **1**. (c) π–π interactions between two adjacent chains shown as green lines. (d) Hydrogen bonding interactions formed around the free water molecule shown as green dashed lines. Co, cyan or polyhedrons; O, red; N, blue; C, black; H, gray. (For interpretation of the references in color in this figure legend, the reader is referred to the web version of this article.)

groups adopt μ_1-η^1:η^1 chelating mode and another two carboxylate groups adopt μ_1-η^1:η^0 mode, forming a 1D polymeric chain of ladder shape extended along the *b* axis with the adjacent Co–Co distance of 5.657 Å (Fig. 1(b)). In the lattice, π–π interactions and hydrogen bonding interactions are simultaneously observed between interchain to generate a 3D structure. The π–π interactions of the DBI ligands (3.725 and 3.807 Å) connect the nearest alternating chain along *c* axis (Fig. 1(c)), and then hydrogen bonding interactions of O(5)–H(5A)···O(4) (2.829 Å), O(5)–H(5B)···O(3) (2.842 Å), N(4)–H(4)···O(5) (2.889 Å) and N(5)–H(5)···O(5) (2.770 Å) further connect the 2D layer along *b* axis to form a 3D supramolecular framework (Fig. 1(d)).

3.3. Crystal structure of $[Co(PDA)(DBI)\cdot(H_2O)]_n$ (**2**)

2 crystallizes in monoclinic space group *C*2/*c*. Co(II) ion is surrounded by four oxygen atoms from three individual PDA^{2-} ligands, one nitrogen atom from DBI and one oxygen atom from one water molecule in a slightly distorted octahedral coordination geometry, as shown in Fig. 2(a). The bond distance of Co(1)–N(1) is 2.104(2) Å and Co–O bond lengths are in the range of 2.065(2) and 2.226(2) Å which are a little longer than those of **1**. These bonds are comparable to reported values [29–31]. The O–Co–O and O–Co–N angles range from 60.16° to 175.75°. One carboxylate group adopts the μ_1-η^1:η^1 chelating mode and the other μ_2–η^1:η^1 bridging mode in a *syn-anti* fashion. The μ_2-carboxylates linked two Co(II) ions to form a 1D zig–zag chain. The distance of neighboring Co(II) ions is 5.282 Å. All PDA^{2-} ligands adopt the same mode linking three Co(II) ions to give a 2D layer structure (Fig. 2(b)). The nearest distance of neighboring Co(II) ions from the alternating chains is 5.724 Å. Hydrogen bonds were also found in O(5)–H(5A)···O(1) (2.679 Å) and O(5)–H(5B)···O(3) (2.691 Å). The π–π interactions of the DBI ligands from adjacent 2D layers were found and further connected the layers to 3D structure (Fig. 2(c)).

3.4. Magnetic properties of **1** and **2**

The temperature-dependent magnetic susceptibilities of **1** and **2** were measured at 1 kOe in the temperature range of 2–300 K. The χ_mT value at 300 K is 2.57 cm^3 mol^{-1} K for **1** and 3.28 cm^3 mol^{-1} K for **2**, which are both higher than the spin-only value of 1.87 cm^3 mol^{-1} K expected for one uncoupled tetrahedral and octahedral high-spin Co(II) ions ($S = 3/2$, $g = 2$) [32]. As *T* decreasing, the χ_mT values continuously decreases to 1.36 cm^3 mol^{-1} K for **1** and 1.16 cm^3 mol^{-1} K for **2**. The magnetic susceptibilities of the two coordination polymers both obey the Curie–Weiss law in the range of 50–300 K with $C = 2.64$ cm^3 mol^{-1} K, $\theta = -7.74$ K for **1** and $C = 3.63$ cm^3 mol^{-1} K, $\theta = -30.35$ K for **2** (Fig. S3). The moderate negative θ values may come from the existence of antiferromagnetic exchange interactions and/or spin-orbital coupling.

The *C* and θ values are observed for other Co(II) coordination polymers with different geometric conformations. A similar result was obtained for octahedral system in Co$_2$(2,5-diphenylterephtha-

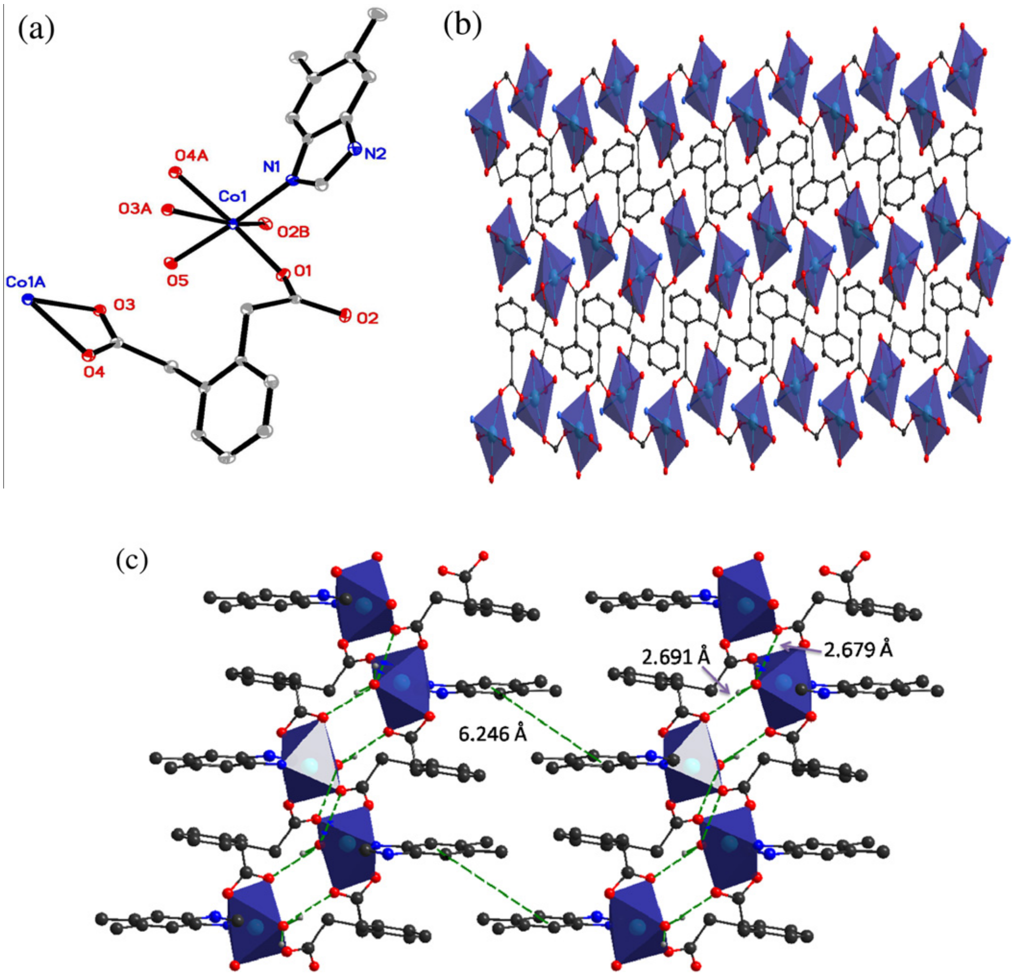

Fig. 2. (a) The coordination environment of Co(II) ions in **2**. (b) The 2D layer structure of **2**. DBI ligands are omitted for clarity. (c) Intrachain hydrogen bonding interactions and π–π interactions between two adjacent layers. Co, polyhedrons; O, red; N, blue; C, black. (For interpretation of the references in color in this figure legend, the reader is referred to the web version of this article.)

late)$_2$(H$_2$O)$_2$ [33]. The susceptibility ($C = 3.12\ \mathrm{cm^3\ K\ mol^{-1}}$ and $\theta = -28.2$ K) suggests weak antiferromagnetic coupling within the chain. Another similar conclusion was reported for {[Co(dpyo)(1,4-bdc)(H$_2$O)$_2$][Co(H$_2$O)$_6$](1,4-bdc)·H$_2$O}, dpyo = 4,4′-bipyridyl *N*,*N*′-oxide [34]. However, when the environment of Co(II) ion is heavily distorted from an octahedron these values can show major deviations. For a tetrahedral Co(II) ion, as found in Co$_2$(2,2′-bpdc)$_2$(dpa)$_2$, where bpdc is biphenyldicarboxylate, $C = 2.47\ \mathrm{cm^3\ K\ mol^{-1}}$ and $\theta = -1.2(2)$ K [35]. From the comparison of these simple cases that for tetrahedral system we usually find the expected values while for octahedral systems the absolute values are much higher, especially θ values.

Since the environment of the high-spin Co(II) ion for **1** is tetrahedral, zero field splitting of the $^4A_2$ ground state may play a major effect with the quenched orbital momentum. The magnetic susceptibility data were first treated by a mononuclear Co(II) mode in the crystal field, then magnetic interactions between the Co(II) ions are further considered as a molecular field approximation. The total equation is

$$\chi_{\parallel} = \frac{N\beta^2 g_z^2}{4kT} \times \frac{1 + 9\exp(-2D/kT)}{1 + \exp(-2D/kT)}$$
$$\chi_{\perp} = \frac{N\beta^2 g_x^2}{kT} \times \frac{1 + (\frac{4}{3}x)[1 - \exp(-2x)]}{1 + \exp(-2x)} \qquad (x = D/kT)$$
$$\chi_{co} = (\chi_{\parallel} + 2\chi_{\perp})/3$$
$$\chi_M = \chi_{Co}/[1 - \chi_{Co}(2zJ'/Ng^2\beta^2)] \tag{1}$$

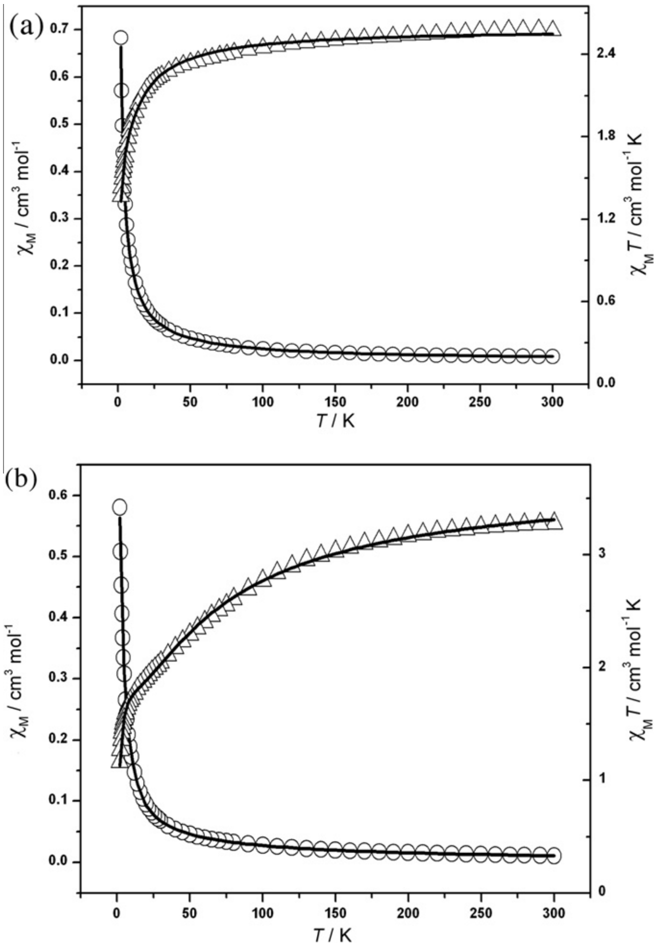

Fig. 3. Plots of χ_m (O) and $\chi_m T$ (△) vs. T for **1**(a) and **2**(b). The solid line denotes the theoretical fit of the experimental data.

The best fit (as shown in Fig. 3(a)) using a least-squares analysis led to $D = -0.47\ \mathrm{cm^{-1}}$, $g = 2.30$, $zJ' = -0.48\ \mathrm{cm^{-1}}$ and $R = 1.6 \times 10^{-4}$. The negative zJ' value indicates weak antiferromagnetic interactions between Co(II) ions.

A similar attempt was also performed to the data of **2**, but the result is not satisfactory. The magnetic data of **2** were fitted by using a simple phenomenological Eq. (2) [36–38],

$$\chi_M T = A\exp(-E_1/kT) + B\exp(-E_2/kT) \tag{2}$$

Here, $A + B$ equals the Curie constant, and E_1, E_2 represent the ‘activation energies’ corresponding to the spin–orbit coupling and the magnetic exchange interaction, respectively. The fitting of the experimental data using this model (as shown in Fig. 3(b)) gives $A + B = 3.42\ \mathrm{cm^3\ mol^{-1}\ K}$, $-E_1/k = -103.75$ K, $-E_2/k = -1.6$ K with $R = 8.1 \times 10^{-5}$. The $A + B$, $-E_1/k$ and $-E_2/k$ values of the complex are of the same magnitude as those values in previously reported cobalt complexes [36–39]. The $-E_2/k$ value of -1.6 K is corresponding to $J = -3.2$ K according to the Ising chain approximation, which indicates antiferromagnetic interactions of Co(II) ions in **2**. The magnetic interactions of Co(II) ions in **2** is much stronger than **1**, which is consistent with the different bridge ligands (the bridge of **2** is Co···O–C–O···Co, and that of **1** is Co···O–(C)$_{4or5}$–O···Co).

4. Conclusion

Two new Co(II) coordination polymers with 5,6-dimethyl-1*H*-benzoimidazole and aromatic carboxylic acid were synthesized and characterized. **1** exhibits 1D ladder-like chain linked by BTA^{4-} ions, which further assemble into 3D supermolecular structure through π–π interactions and hydrogen bond interactions, while **2** shows a 2D layer linked by carboxylate groups. The magnetic studies revealed the presence of antiferromegnetic interactions between the adjacent Co(II) ions.

Acknowledgement

This work was support by the National Natural Science Foundation of China (No. 20801028), the NSF of Tianjin (Nos. 09JCYBJC04000 and 08ZCGHHZ01100), MOE (No. 20070055046) of China, and the National Innovation Projects for the Undergraduates of China.

Appendix A. Supplementary material

CCDC 743079 and 743080 contain the supplementary crystallographic data for this paper. These data can be obtained free of charge from The Cambridge Crystallographic Data Centre via www.ccdc.cam.ac.uk/data_request/cif. Supplementary data associated with this article can be found, in the online version, at doi:10.1016/j.ica.2010.05.041.

References

[1] B. Moulton, M.J. Zaworotko, Chem. Rev. 101 (2001) 1629.
[2] K. Tanaka, F. Toda, Chem. Rev. 100 (2000) 1025.
[3] L. Carlucci, G. Ciani, D.M. Proserpio, Coord. Chem. Rev. 246 (2003) 247.
[4] D. Parkar, Coord. Chem. Rev. 205 (2000) 109.
[5] J.D. Dunitz, Pure Appl. Chem. 63 (1991) 177.
[6] O. Ikkala, G. Brinke, Science 295 (2002) 2407.
[7] J.-P. Zhang, Y.-Y. Lin, W.-X. Zhang, X.-M. Chen, J. Am. Chem. Soc. 127 (2005) 14162.
[8] P.G. Van Patten, A.P. Shreve, J.S. Lindsey, R.J. Donohoe, J. Phys. Chem. B 102 (1998) 4209.
[9] N.L. Toh, M. Nagarathinam, J.J. Vittal, Angew. Chem., Int. Ed. 44 (2005) 2237.
[10] B.F. Hoskins, R. Robson, D.A. Slizys, J. Am. Chem. Soc. 119 (1997) 2952.
[11] M. Eddaoudi, J. Kim, N. Rosi, D. Vodak, J. Wachter, M. O'Keeffe, O.M. Yaghi, Science 295 (2002) 469.
[12] X.-Y. Wang, S.C. Sevov, Inorg. Chem. 47 (2008) 1037.

[13] Y.-Z. Zhang, W. Wernsdorfer, F. Pan, Z.-M. Wang, S. Gao, Chem. Commun. 47 (2006) 3302.
[14] X.-M. Zhang, Z.-M. Hao, W.-X. Zhang, X.-M. Chen, Angew. Chem., Int. Ed. 119 (2007) 3526.
[15] J.S. Griffith, The Theory of Transition-Metal Ions, Cambridge University Press, 1964.
[16] M. Kurmoo, Chem. Soc. Rev. 38 (2009) 1353.
[17] Y. Oka, K. Inoue, Chem. Lett. 33 (2004) 402.
[18] M. Murrie, S.J. Teat, H.S. Evans, H.U. Güdel, Angew. Chem., Int. Ed. 42 (2003) 4653.
[19] A. Caneschi, D. Gatteschi, N. Lalioti, C. Sangregorio, R. Sessoli, G. Venturi, A. Vindigni, A. Rettori, M.G. Pini, M.A. Novak, Angew. Chem., Int. Ed. 40 (2001) 1760.
[20] C.A. Salata, M.T. Youinou, C.J. Burrows, J. Am. Chem. Soc. 111 (1989) 9278.
[21] Y.-L. Liu, V. Kravtsov, R.D. Walsh, P. Poddar, H. Srikanthc, M. Eddaoudi, Chem. Commun. (2004) 2806.
[22] C.J. Harding, Q. Lu, J.F. Malone, D.J. Marrs, N. Martin, V. Mckee, J. Nelson, J. Chem. Soc., Dalton Trans. (1995) 1739.
[23] P.M. Forster, N. Stock, A.K. Cheetham, Angew. Chem., Int. Ed. 44 (2005) 7608.
[24] P. Mahata, M. Prabu, S. Natarajan, Inorg. Chem. 47 (2008) 8451.
[25] G.M. Sheldrick, SHELXS 97, Program for the Solution of Crystal Structures, University of Göttingen, Germany, 1997.
[26] G.M. Sheldrick, SHELXL 97, Program for the Refinement of Crystal Structures, University of Göttingen, Germany, 1997.
[27] G.H. Wei, J. Yang, J.F. Ma, Y.Y. Liu, S.L. Li, L.P. Zhang, Dalton Trans. (2008) 3080.
[28] Y. Yan, C.D. Wu, X. He, Y.Q. Sun, C.Z. Lu, Cryst. Growth Des. 5 (2005) 821.
[29] J. Li, T. Yuen, C.L. Lin, Inorg. Chem. 38 (1999) 2695.
[30] J. Zhang, Z.J. Li, Y. Kang, J.K. Cheng, Y.G. Yao, Inorg. Chem. 43 (2004) 8085.
[31] G.L. Miessler, D.A. Tarr, Inorganic Chemistry, third ed., Pearson Prentice Hall, 2004.
[32] R.L. Carlin, Magnetochemistry, Springer-Verlag, Berlin, Heidelberg, 1986.
[33] J. Ehrhart, J.M. Planeix, N. Kyritsakas, M.W. Hosseini, Dalton Trans. 32 (2009) 6309.
[34] S.C. Manna, E. Zangrando, J. Ribas, N.R. Chaudhuri, Dalton Trans. 14 (2007) 1383.
[35] H. Kumagai, M. Akita-Tanaka, S. Kawata, K. Inoue, C. J. Kepert, M. Kurmoo, Cryst. Growth Des, submitted for publication.
[36] J.M. Rueff, N. Masciocchi, P. Rabu, A. Sironi, A. Skoulios, Eur. J. Inorg. Chem. (2001) 2843.
[37] S.C. Manna, A.K. Ghosh, J. Ribas, M.G.B. Drew, C.N. Lin, E. Zangrando, N.R. Chaudhuri, Inorg. Chim. Acta 359 (2006) 1395.
[38] J.M. Rueff, N. Masciocchi, P. Rabu, A. Sironi, A. Skoulios, Chem. Eur. J. 8 (2002) 1813.
[39] D. Ghoshal, G. Mostafa, T.K. Maji, E. Zangrando, T.H. Lu, J. Ribas, N.R. Chaudhuri, New J. Chem. 28 (2004) 1204.